ECOLOGY LETTERS

Ecology Letters, (2013) **16**: 371–379 doi: 10.1111/ele.12052

LETTER

Unimodal size scaling of phytoplankton growth and the size dependence of nutrient uptake and use

Emilio Marañón,[1]* Pedro Cermeño,[1] Daffne C. López-Sandoval,[1] Tamara Rodríguez-Ramos,[1] Cristina Sobrino,[1] María Huete-Ortega,[1] José María Blanco[2] and Jaime Rodríguez[2]

Abstract

Phytoplankton size structure is key for the ecology and biogeochemistry of pelagic ecosystems, but the relationship between cell size and maximum growth rate (μ_{max}) is not yet well understood. We used cultures of 22 species of marine phytoplankton from five phyla, ranging from 0.1 to 10^6 μm^3 in cell volume (V_{cell}), to determine experimentally the size dependence of growth, metabolic rate, elemental stoichiometry and nutrient uptake. We show that both μ_{max} and carbon-specific photosynthesis peak at intermediate cell sizes. Maximum nitrogen uptake rate (V_{maxN}) scales isometrically with V_{cell}, whereas nitrogen minimum quota scales as $V_{cell}^{0.84}$. Large cells thus possess high ability to take up nitrogen, relative to their requirements, and large storage capacity, but their growth is limited by the conversion of nutrients into biomass. Small species show similar volume-specific V_{maxN} compared to their larger counterparts, but have higher nitrogen requirements. We suggest that the unimodal size scaling of phytoplankton growth arises from taxon-independent, size-related constraints in nutrient uptake, requirement and assimilation.

Keywords

Carbon, growth rate, nitrogen, nitrogen maximum uptake rate, photosynthesis, phytoplankton, respiration, size scaling, stoichiometry.

Ecology Letters (2013) **16**: 371–379

INTRODUCTION

The decrease in maximum intrinsic population growth rate (μ_{max}) and mass-specific metabolic rates (R^M) with increasing body size (M) is one of the most pervasive patterns in biology (Fenchel 1974) and has major implications for the ecology and evolution of all organisms (Brown *et al.* 2004). Numerous studies have shown that μ_{max} and R^M of plants and metazoans scale as $M^{-1/4}$, which derives from the fact that individual metabolic rates scale as $M^{3/4}$, as a result of the biophysical limitations imposed by resource transportation networks as body size increases (Banavar *et al.* 2002). It is not clear, however, whether a single, scale-free model can capture adequately all the factors that govern individual metabolism and population growth across wide body-size and phylogenetic ranges (Kolokotrones *et al.* 2010). In particular, the applicability of the ¾-power rule to unicellular organisms has often been questioned (Sommer 1989; Marañón *et al.* 2007; Marañón 2008; Johnson *et al.* 2009; Huete-Ortega *et al.* 2012).

Phytoplankton, a polyphyletic group of photosynthetic, unicellular organisms that live in the surface of all aquatic ecosystems, dominate marine primary production and are responsible for nearly half of the annual CO_2 fixation on Earth (Falkowski & Oliver 2007). Understanding the size scaling of growth and metabolic rate in these organisms is especially relevant because phytoplankton size structure is a key property of planktonic communities, which determines their potential to sustain upper trophic levels, export organic carbon into the deep ocean and sequester atmospheric CO_2 (Legendre & Rassoulzadegan 1996; Falkowski & Oliver 2007). Species with fast growth rates can be expected to dominate phytoplankton blooms, events of enhanced biomass and productivity that result from transient situations of high resource availability and contribute disproportionately to biogeochemical fluxes.

There is a large variability in the reported size scaling of phytoplankton growth and metabolic rate (Finkel *et al.* 2010). Using the same metric to describe cell size (e.g. cell volume), some studies support the size dependence predicted by the general allometric model (Banse 1976; Blasco *et al.* 1982), whereas others suggest a weaker (Banse 1982; Chisholm 1992; Marañón *et al.* 2007; Huete-Ortega *et al.* 2012) or a stronger (Taguchi 1976; Finkel 2001) degree of size dependence. This variability probably results from lack of methodological consistency among studies, differences in the range of cell sizes and taxonomic groups studied, as well as the influence of resource availability upon metabolic activity (Finkel *et al.* 2004). Most analyses of the size scaling of phytoplankton growth rate have not been accompanied by direct measurements of the metabolic properties that control biomass production and population growth, such as nutrient uptake and assimilation, carbon fixation and elemental stoichiometry. Conversely, the few studies that did address some of those properties (Taguchi 1976; Blasco *et al.* 1982; Finkel 2001) did not cover the full range of phytoplankton cell size and were restricted to a single taxonomic group. Conclusive evidence is thus lacking both on the nature of the size scaling of phytoplankton growth and metabolic rates as well as on the role of the different underlying mechanisms.

Phytoplankton growth requires the acquisition of nutrients and their assimilation, or conversion into biomass, to form new cells. Following Droop's model, and assuming there is no mortality, phytoplankton growth rate (μ) can be described as a function of the cellular quota of the limiting nutrient (Q) and the minimum nutrient quota (Q_{min}), below which cells cannot grow (Droop 1973):

[1]*Departamento de Ecología y Biología Animal, Universidad de Vigo, 36210, Vigo, Spain*

[2]*Departamento de Ecología, Universidad de Málaga, 29071, Málaga, Spain*

**Correspondence: E-mail: em@uvigo.es*

$$\mu = \mu_\infty \left(1 - \frac{Q\min}{Q}\right), \quad (1)$$

where μ_∞ is the theoretical maximum growth rate when Q is infinite. The realised maximum growth rate (μ_{max}) is attained, under nutrient-saturated conditions, when Q reaches its maximum, Q_{max}. The variability in Q over time is given by the balance between nutrient uptake rate (V) and nutrient assimilation ($N_{assim} = \mu\, Q$) into biomass (Droop 1973):

$$\frac{dQ}{dt} = V - \mu Q \quad (2)$$

V depends on external nutrient concentration and the nutrient half-saturation constant, following Michaelis–Menten kinetics. The nutrient-saturated uptake rate is an inverse function of the excess quota, $Q - Q_{min}$, such that it approaches V_{max}, the maximum nutrient uptake rate, when Q is close to Q_{min}, but decreases as cells fill up with nutrients and Q approaches Q_{max} (Gotham & Rhee 1981). Hence, size-related differences in the storage capacity, Q_{maxN}/Q_{minN}, can affect the time scale over which different species can sustain high rates of nutrient uptake (Verdy *et al.* 2009).

Taking into account the conceptual framework described above, we determined experimentally the size scaling of phytoplankton growth and metabolic rate across a cell-size range of more than seven orders of magnitude using cultures of 22 species from five phyla. We also analysed the size scaling of carbon and nitrogen quotas, maximum nutrient uptake rate and nutrient assimilation and storage to understand the physiological mechanisms that underlie the observed size dependence of phytoplankton growth. Because μ_{max} is a key determinant of fitness, our analysis serves to define size-dependent ecological strategies and provides insight into the assembly and dynamics of phytoplankton communities in the ocean.

MATERIAL AND METHODS

Culture maintenance

We grew monocultures of 22 phytoplankton species ranging in cell size from 0.12 to 2 500 000 μm^3 and belonging to seven classes from five phyla (Table 1; Table S1). Cultures were obtained from Provasoli–Guillard National Center for Marine Algae (USA), Roscoff Culture Collection (France), Culture Collection of Algae and Protozoa (UK), Instituto Español de Oceanografía (Spain) and Estación de Ciencias Mariñas de Toralla (Spain). All equipment used for medium preparation and culturing were previously soaked in 10% HCl during 48 h, then rinsed thoroughly with ultrapure, deionized water and finally autoclaved at 120 °C for 60 min. Growth media were prepared with autoclaved, 0.2-μm-filtered seawater. We used the f/4 medium for most species, with the silicate excluded in the case of non-diatoms, and additional trace metals (L1 trace element solution) added in the case of dinoflagellates. *Ostreococcus tauri* and *Micromonas pusilla* were grown on K/2 medium, whereas *Prochlorococcus* sp. was grown on PCR-S11/2 medium. In all cases, the concentration of dissolved inorganic nitrogen (NH_4^+ for *Prochlorococcus* sp., NO_3^- for all other species) was reduced by fourfold, so that the N/P molar ratio was *c.* 6 and nitrogen limitation was ensured during the stationary phase.

Cultures were maintained in a culture chamber at 18 ± 0.5 °C and illuminated with cool white light at a photon flux of 250 μmol photons m^{-2} s^{-1} [Biospherical QSL-2100 spherical quantum sensor (Biospherical Instruments Inc., San Diego, CA, USA)] in a 12L : 12D photoperiod. The irradiance used was likely to be saturating for both photosynthesis and growth (Langdon 1987; Cullen *et al.* 1992). Aeration was used in all species except the dinoflagellates. Air was supplied through a 0.45-μm filter from outside the culture chamber. Cultures were acclimated in 1-L flasks before conducting measurements. After first inoculating the medium with 5–10 mL of stock culture, the population was allowed to grow until it reached the late exponential growth phase, when an aliquot was transferred to fresh medium and again allowed to reach the late exponential growth phase. This procedure was repeated three times, to ensure acclimation of each species to the growth conditions. During the last growth cycle, which was carried out in 4-L flasks, populations were allowed to reach the stationary phase (see Figs. S1–S5). During this last growth cycle, samples for the determination of standing stocks were collected daily and metabolic rates were determined during the exponential growth phase.

Standing stocks

Cultures were sampled daily to determine cell abundance, chlorophyll *a* concentration, particulate organic carbon (POC) and particulate organic nitrogen (PON) and dissolved inorganic nitrogen. Cell abundance and biovolume of *Prochlorococcus* sp., *Synechococcus* sp., *O. tauri* and *M. pusilla* were determined using a FACScan flow cytometer (Becton Dickinson, Franklin Lakes, NJ, USA) following the methods detailed elsewhere (Huete-Ortega *et al.* 2012). For the other species, cell counts were performed under the microscope using Neubauer or Sedgewick-Rafter counting chambers, with the exception of the two *Coscinodiscus* species, whose abundance was determined after sedimentation of 10-mL samples in an Utermöhl chamber. Biovolume was measured using a Leica DLMB (Leica Microsystems GmbH, Wetzlar, Germany) microscope using the NIS-Elements BR 3.0 image analysis software (Nikon Instruments Inc., Melville, NY, USA). Critical cell dimensions were obtained in at least 100 cells and biovolume was calculated using the appropriate geometric shapes (Huete-Ortega *et al.* 2012). The maximum intrinsic growth rate (μ_{max}) was determined for each species during the exponential growth phase, when both nutrients and irradiance were non-limiting. We calculated μ_{max} as the slope in the linear regression of the natural logarithm of cell abundance vs. time (days). The r^2 of this linear regression during the exponential growth phase was always > 0.9.

Chlorophyll *a* concentration was measured fluorometrically on a TD-700 Turner fluorometer after filtration of duplicate 5-mL samples onto GF/F filters, freezing of the filters at −20 °C and extraction with 90% acetone. For POC and PON determination, duplicate 10-mL samples were filtered onto pre-combusted GF/F filters, which were stored at −20 °C. Prior to analysis, filters were kept in a desiccator at room temperature for 48 h. Samples were analysed using a Carlo Erba Instruments EA 1108 elemental analyser (CE Instruments Ltd, Wigan, UK) using an acetanilide standard as a reference. By dividing POC and PON by cell density, we obtained the carbon and nitrogen cell quotas. We calculated the maximum (Q_{maxN}) and minimum (Q_{minN}) nitrogen quotas as the highest and lowest nitrogen cell content measured throughout the

Table 1 Cell size, composition, growth and metabolic rates for each phytoplankton species. Variables are cell volume (V_{cell}), cell carbon (C_{cell}), minimum nitrogen quota (Q_{minN}), maximum nitrogen quota (Q_{maxN}), mean C : N ratio, maximum nitrogen uptake rate (V_{maxN}), carbon-specific total photosynthesis rate (P^C), carbon-specific respiration rate (R^C), percentage of extracellular release (PER), photosystem II maximum quantum efficiency (F_v/F_m) and maximum population growth rate (μ_{max}). V_{cell}, C_{cell}, P^C, R^C, PER, F_v/F_m and μ_{max} were measured during the exponential growth phase. V_{maxN} was determined during the stationary phase. The mean C : N ratio was computed from daily measurements ($n \geq 6$) obtained throughout the growth cycle. *N.A.*, data not available

Species	V_{cell} μm^3 $cell^{-1}$	C_{cell} pgC $cell^{-1}$	Q_{minN} pgN $cell^{-1}$	Q_{maxN} pgN $cell^{-1}$	C:N at:at	V_{maxN} pgN $cell^{-1}$ h^{-1}	P^C h^{-1}	R^C h^{-1}	PER (%)	F_v/F_m	μ_{max} d^{-1}
Prochlorococcus sp.	0.12	0.035	0.011	0.021	3.3	6.37E-05	0.019	0.0017	1.5	0.45	0.28
Synechococcus sp.	0.41	0.094	0.019	0.039	5.4	4.06E-04	0.035	0.0043	2.0	*N.A.*	0.30
Ostreococcus tauri	2.4	0.67	0.16	0.31	5.1	4.72E-03	0.035	0.0020	2.8	0.62	0.41
Nannochloropsis gaditana	8.6	1.8	0.40	0.74	6.1	2.25E-02	0.074	0.0055	1.2	0.57	0.49
Micromonas pusilla	11	2.5	0.43	0.77	4.3	9.67E-03	0.074	0.0073	8.0	0.59	0.59
Pavlova lutheri	45	6.0	0.55	2.2	9.8	3.31E-02	0.136	0.0074	1.0	0.62	0.70
Calcidiscus leptoporus	51	5.4	0.48	2.2	7.0	6.79E-02	*N.A.*	0.0034	*N.A.*	0.67	0.89
Isochrysis galbana	64	4.3	0.58	1.4	7.8	4.11E-02	0.101	0.0067	0.6	0.68	0.82
Gephyrocapsa oceanica	82	12	1.8	6.6	6.7	9.85E-02	0.166	0.0050	1.2	0.66	0.85
Phaeodactylum tricornutum	93	5.2	0.31	1.4	7.2	3.63E-02	0.205	0.0026	0.3	0.63	1.06
Emiliania huxleyi	158	7.8	0.68	2.2	10.0	8.70E-02	0.115	0.0036	0.3	0.64	0.92
Skeletonema costatum	242	26	2.9	5.0	9.4	3.35E-01	0.143	0.0036	0.1	*N.A.*	0.85
Thalassiosira weissflogii	1163	55	6.4	21	8.4	3.09E-01	0.119	0.0026	0.3	0.69	0.54
Melosira nummuloides	2285	269	35	115	9.0	4.52E+00	*N.A.*	0.0021	*N.A.*	0.62	0.56
Protoceratium reticulatum	2383	920	116	357	7.4	1.45E+01	0.052	0.0042	2.9	0.61	0.43
Thalassiosira rotula	2597	195	21	88	11.9	1.12E+00	0.071	0.0031	0.5	0.62	0.60
Alexandrium minutum	5575	1106	73	262	8.6	5.03E+00	0.027	0.0067	7.2	0.60	0.33
Akashiwo sanguinea	47349	2555	392	1093	6.6	1.18E+02	0.047	0.0082	7.8	0.50	0.34
Dytilum brightwellii	75827	3484	275	940	6.1	1.99E+01	0.052	0.0034	2.3	0.60	0.32
Coscinodiscus radiatus	81955	3939	773	3387	6.0	1.96E+02	0.023	0.0028	1.2	0.65	0.35
Alexandrium tamarense	88836	1452	155	683	7.9	1.31E+01	0.039	0.0104	4.2	0.57	0.24
Coscinodiscus wailesii	2498458	85860	10495	48032	8.0	9.46E+02	0.054	0.0053	5.4	0.71	0.25

growth cycle. For dissolved inorganic nutrient analysis, 10-mL samples, previously filtered through 0.45-μm polycarbonate filters, were frozen at −80 °C and then analysed using a segmented-flow Skalar autoanalyser, following standard colorimetric methods.

Metabolic activity

We determined daily the photosystem II maximum photochemical efficiency (F_v/F_m). Triplicate, 5-mL samples were acclimated in the dark for 30 min and then F_v/F_m was determined using a Pulse Amplitude Modulated [Water PAM; Walz (Heinz Walz GmbH, Effeltrich, Germany)] fluorometer. During the exponential growth phase (see Figs. S1–S5), we also measured the rates of photosynthesis and respiration. Photosynthetic CO_2 fixation was measured with the $^{14}CO_2$ uptake technique, using the filtrate recovery protocol to determine the production of both particulate and dissolved organic carbon. Five 20-mL samples (three light and two dark bottles) received 1–5 μCi of $NaH^{14}CO_3$ and were incubated for 2 h in the same incubation chamber where the cultures were kept. Filtration and processing of samples, as well as data calculations, were carried out as described elsewhere (Marañón *et al.* 2004). Total photosynthetic carbon fixation was calculated as the sum of the particulate and dissolved organic carbon production. The percentage of extracellular release (PER) was calculated by dividing dissolved organic carbon production by total carbon fixation. Respiration was measured as the rate of O_2 consumption during incubations in the dark. Six 50-mL borosilicate bottles were filled with culture. Three bottles were fixed immediately to determine the initial oxygen concentration, whereas the remaining three bottles were incubated for 24 h. Oxygen concentration was then measured in all bottles using the Winkler technique with a potentiometric endpoint. Oxygen consumption rates were converted into carbon units by assuming that the O_2 consumption to CO_2 production ratio was 1.4 (mol : mol).

During the stationary phase, when populations were nitrogen limited, we determined the maximum rate of dissolved inorganic nitrogen uptake (V_{maxN}). We prepared a series of culture aliquots to which different amounts of nitrate (ammonium in the case of *Prochlorococcus* sp.) were added. Thereafter, samples for dissolved inorganic nitrogen concentration in the bulk medium were taken at different time intervals (0, 5, 10, 15, 20, 30, 45 min) and processed as described above. The nutrient uptake rate for each aliquot was calculated as the slope of the linear regression of nutrient concentration over time, and V_{maxN} was taken as the highest slope value obtained. We also estimated the mean cell-specific rate of nutrient uptake during the exponential growth phase (V_{expN}). V_{expN} was computed from the daily decrease in dissolved inorganic nitrogen measured in the culture medium. Finally, nitrogen assimilation rate (N_{assim}) was calculated as $\mu_{max} \times Q_{expN}$, where Q_{expN} is the mean nitrogen quota during the period of exponential growth.

RESULTS

Growth and metabolic rate

We found that the relationship between μ_{max} and cell size is unimodal (Fig. 1a, Table 1). μ_{max} decreased with increasing cell size only for species larger than *c.* 50–100 μm^3; below this size range, it increased with cell size. μ_{max} was 0.2–0.4 day^{-1} in both large and small species, whereas it took values above 0.8 day^{-1} in intermediate-size (*c.* 100 μm^3) species. The log–log relationship between μ_{max}

and cell volume (V_{cell}) had a slope of 0.19 and −0.15 for small-to-medium and medium-to-large species, respectively, both relationships being highly significant (Table 2). The size scaling of μ_{max} was largely independent of taxonomic affiliation, as all species studied, despite their belonging to different phylogenetic groups, conformed to the overall unimodal pattern. The decrease in μ_{max} with increasing cell size was observed both in diatoms and dinoflagellates, whereas the increase in μ_{max} with increasing cell size took place in cyanobacteria, chlorophytes and other flagellate species. The same unimodal pattern was also found in the relationship between carbon-specific photosynthesis rate (P^C) and cell size: intermediate-size species showed P^C values of 0.1–0.2 h^{-1}, whereas in both small and large species, P^C was below 0.05 h^{-1} (Fig. 1b). The log–log relationship between P^C and V_{cell} had a slope of 0.30 and −0.20 in small-to-medium and medium-to-large species, respectively, and both relationships were highly significant (Table 2). Carbon-specific respiration rates (R^C) ranged between 0.002 and 0.010 h^{-1} and, in contrast to μ_{max} and P^C, did not show any size dependence (Fig. 2a). The relative importance of respiration, expressed as the respiration-to-photosynthesis ratio, was < 15% in most species and showed even lower values (< 5%) in intermediate-size species (Fig. 2b). The release in dissolved form of recently fixed organic carbon was unimportant, as the PER generally took values below 5% (average: 2.5%; range: 0.1–8.0%) and was not related to cell size (Table 1).

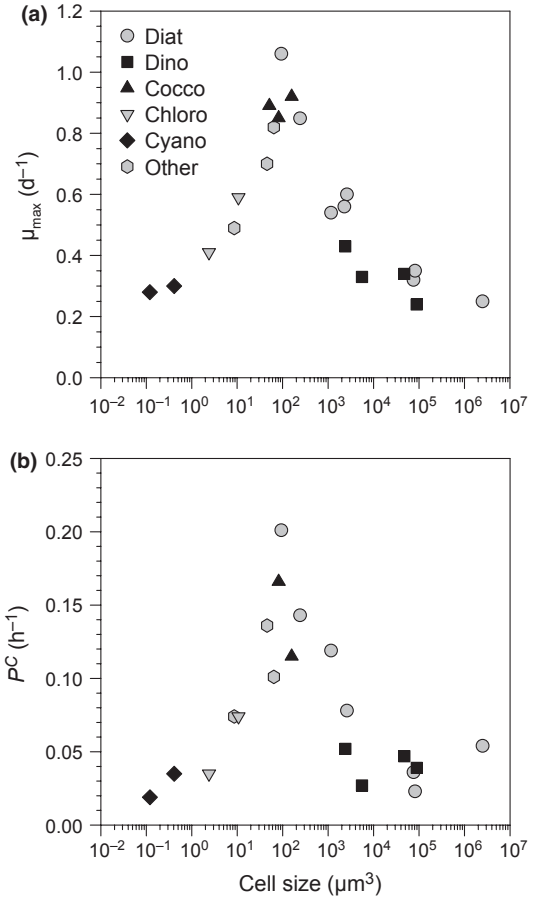

Figure 1 Size scaling of growth and metabolic rate. Cell-size dependence of (a) maximum growth rate and (b) biomass-specific CO_2 fixation in 22 species of phytoplankton including diatoms (Diat), dinoflagellates (Dino), coccolithophores (Cocco), chlorophytes (Chloro) and cyanobacteria (Cyano). See Table 1 for data on each individual species.

Nitrogen uptake, assimilation and cell quotas

Despite the fact that species belonged to different phylogenetic groups, cell size alone explained a very high percentage (≥ 95%) of the variability in both maximum nitrogen uptake rate (V_{maxN}) and nitrogen cell quotas (Fig. 3a, b; Table 2). V_{maxN} scaled isometrically with V_{cell}, as the size-scaling slope took a value of 0.97, which was not significantly different from 1 (Table 2). In contrast, the size-scaling slope for the minimum nitrogen cell quota (Q_{minN}) was 0.84 (Fig. 3b; Table 2), while that of the maximum nitrogen cell quota (Q_{maxN}) was 0.93 (Table 2). The log–log relationship between V_{maxN} and Q_{minN} had a slope of 1.15, which was significantly higher than 1 (Fig. 2c; Table 2). The size scaling of V_{expN}, the rate of nutrient uptake during the exponential phase, was the same as that of V_{maxN} (Fig. S6). While V_{maxN} scaled isometrically with V_{cell}, the size scaling of nitrogen assimilation (N_{assim}) was strongly allometric, as the slope of the log–log relationship between N_{assim} and V_{cell} was 0.81 (Table 2), indicating that the rate of conversion of nitrogen into biomass, on a cell-volume basis, decreased with increasing cell size. As a result, the ratio between V_{maxN} and N_{assim} increased markedly with cell size, taking values below 2 in small species and above 3 in most large species (Fig. 3d).

Table 2 Size-scaling parameters for phytoplankton composition, metabolism and growth. Reduced major axis linear regression was used to determine the relationship between log_{10}-transformed variables. N_{assim} is nitrogen assimilation rate. Other abbreviations as in Table 1. Bootstrap confidence limits (95%) are given in parentheses. All regressions were highly significant ($P < 0.01$)

Dependent variable	Units	Independent variable	Slope	95% CI limits	Intercept	95% CI limits	r^2	n	Data set
μ_{max}	day^{-1}	V_{cell}	0.19	0.16, 0.23	−0.43	−0.50, −0.40	0.94	12	Species with V_{cell} < 300 μm³
μ_{max}	day^{-1}	V_{cell}	−0.15	−0.19, −0.12	0.22	0.13, 0.34	0.86	17	Species with V_{cell} > 40 μm³
P^C	h^{-1}	V_{cell}	0.30	0.25, 0.39	−1.45	−1.58, −1.37	0.90	11	Species with V_{cell} < 300 μm³
P^C	h^{-1}	V_{cell}	−0.20	− 0.29, −0.14	−0.44	−0.62, −0.19	0.63	15	Species with V_{cell} > 40 μm³
C_{cell}	pgC $cell^{-1}$	V_{cell}	0.88	0.83, 0.94	−0.69	−0.83, −0.58	0.97	22	All species
V_{maxN}	pgN $cell^{-1}$ h^{-1}	V_{cell}	0.97	0.89, 1.06	−3.00	−3.18, −2.78	0.96	22	All species
Q_{maxN}	pgN $cell^{-1}$	V_{cell}	0.93	0.83, 0.96	−1.26	−1.35, −0.99	0.99	22	All species
Q_{minN}	pgN $cell^{-1}$	V_{cell}	0.84	0.77, 0.92	−1.47	−1.78, −1.26	0.95	22	All species
V_{maxN}	pgN $cell^{-1}$ h^{-1}	Q_{minN}	1.15	1.06, 1.24	−1.29	−1.43, −1.13	0.98	22	All species
N_{assim}	pgN $cell^{-1}$ h^{-1}	V_{cell}	0.81	0.74, 0.88	−2.91	−3.06, −2.69	0.97	22	All species
V_{max} : N_{assim}	unitless	V_{cell}	0.19	0.14, 0.25	−0.18	−0.37, 0.01	0.65	22	All species

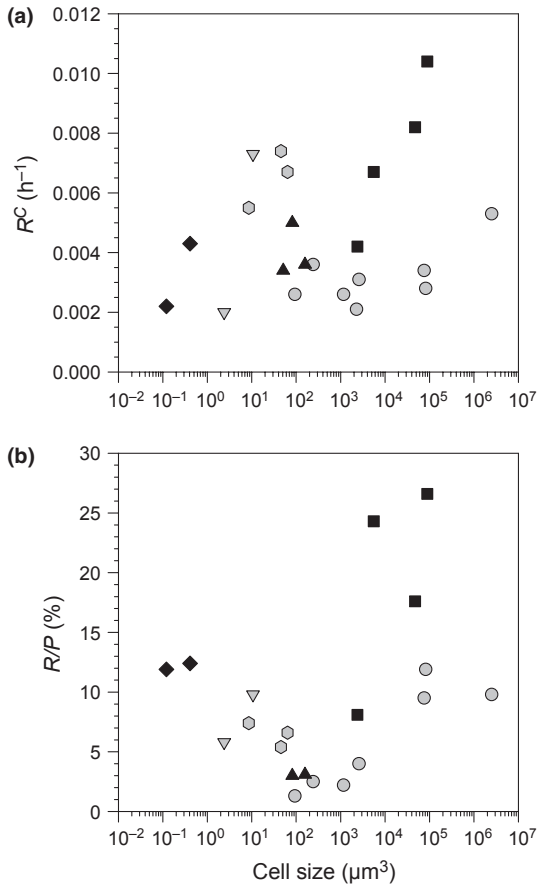

Figure 2 Size scaling of phytoplankton respiration. Cell-size dependence of (a) biomass-specific respiration rate and (b) the respiration-to-photosynthesis ratio. See Table 1 for data on each individual species. Symbols as in Fig. 1.

The different values of the size-scaling slope for Q_{minN} and Q_{maxN} (Table 2) indicate that Q_{maxN} increases with cell size faster than Q_{minN} does. This was also reflected in the fact that the ratio Q_{maxN}/Q_{minN}, which is an indicator of the cells' storage capacity, increased with cell size, taking values around two in small species and values above three in most intermediate-size and large species (Fig. 4a). The carbon-to-nitrogen ratio (C : N) was 7–10 in most intermediate-size and large species, whereas the small species showed markedly lower values (3–6), indicating that they were more nitrogen rich (Fig. 4b).

DISCUSSION

Our study is based on the experimental determination, using fully standardised protocols, of physiological properties of phytoplankton cultures growing under the same conditions. This approach allows us to avoid the uncertainties associated with the analysis of data compiled from the literature, as different studies involve differences in growth conditions and experimental techniques that cannot be easily accounted for. The unimodal pattern in the relationship between cell size and growth and metabolic rate thus appears robust, particularly considering the wide cell size and phylogenetic ranges considered. Previous studies of interspecific size scaling in phytoplankton growth rates (Banse 1982; Sommer 1989; Tang 1995; Finkel 2001) failed to detect this unimodal pattern, probably because they did not cover the picophytoplankton to small nanophytoplankton (0.1–50 μm^3) size range. To understand the mechanisms underlying the unimodal size scaling of phytoplankton growth, we need to focus on the size scaling of carbon and nitrogen metabolism and stoichiometry.

Because population growth requires the synthesis of new biomass, μ_{max} is expected to be closely related to metabolic rate (Fenchel 1974; Brown *et al.* 2004). Indeed, we observed the same unimodal size scaling in carbon-specific CO_2 fixation, which represents a biomass turnover rate. A unimodal size scaling of biomass-specific metabolic rate corresponds to a curvature in the log–log relationship between individual metabolic rate and body size (Kolokotrones *et al.* 2010; Chen & Liu 2011). The presence of this curvature indicates that, when a sufficiently large range in body size is considered, a single, scale-free power law relating metabolic rate with cell size is not applicable to photosynthetic unicells.

It has been suggested that size-related differences in respiratory losses is an important factor explaining the size scaling of phytoplankton growth rates as well as phytoplankton size structure in the ocean (Laws 1975). Our results, as those of other studies (Falkowski & Owens 1978; Langdon 1988), do not support this view. Contrary to photosynthesis, biomass-specific respiration rates did not show any relationship with cell size. In most species, respiratory losses represented a small fraction of total carbon fixation, reflecting near-optimal conditions during the exponential growth phase of our cultures (Geider 1992). As exudation in our cultures was also low and showed no size dependence, our results indicate that phytoplankton μ_{max} and its size scaling is largely controlled by metabolic gains rather than losses. We now examine the size scaling of V_{maxN}, Q_{minN}, Q_{maxN} and $V_{maxN} : N_{assim}$ to assess the potential roles of nutrient uptake, assimilation and storage in controlling the size dependence of μ_{max}.

According to theoretical predictions, and assuming a constant density of transport sites on the cell membrane, V_{maxN} should be linearly related to cell surface area (Aksnes & Egge 1991). This would lead to a scaling exponent of 2/3 between V_{maxN} and V_{cell}, which has been found in a study of eight species covering a size range from 100 to 10 000 μm^3 (Smith & Kalff 1982) and also in several reviews of data from the literature (Litchman *et al.* 2007; Finkel *et al.* 2010). A more recent literature review (Edwards *et al.* 2012) suggests a steeper slope value (0.82), which still would be significantly lower than 1. In contrast, our direct measurements, all conducted under identical conditions and following the same experimental protocols, indicate that V_{maxN} scales isometrically (slope = 0.97) with cell volume, which implies that the rate of nutrient uptake per unit cell surface area increases with cell size, probably as a result of an increasing density of transport sites (Aksnes & Cao 2011). Given that the size-scaling exponent for Q_{minN} was 0.84, V_{maxN} scaled with Q_{minN} with an exponent of 1.15, which is significantly larger than 1. This means that as phytoplankton species become larger, their ability to take up nitrogen, when available in large concentrations, increases faster than their minimum nitrogen requirement does. It also means that as cell size becomes smaller, the maximum nutrient uptake rate decreases faster than the minimum nitrogen requirement. The ability of larger species to sustain high values of V_{maxN} is associated with an increasing storage capacity, which is reflected in the fact that Q_{maxN} has a higher size-scaling exponent than Q_{minN}. The higher storage capacity of larger cells implies that, compared with smaller cells, they fill up

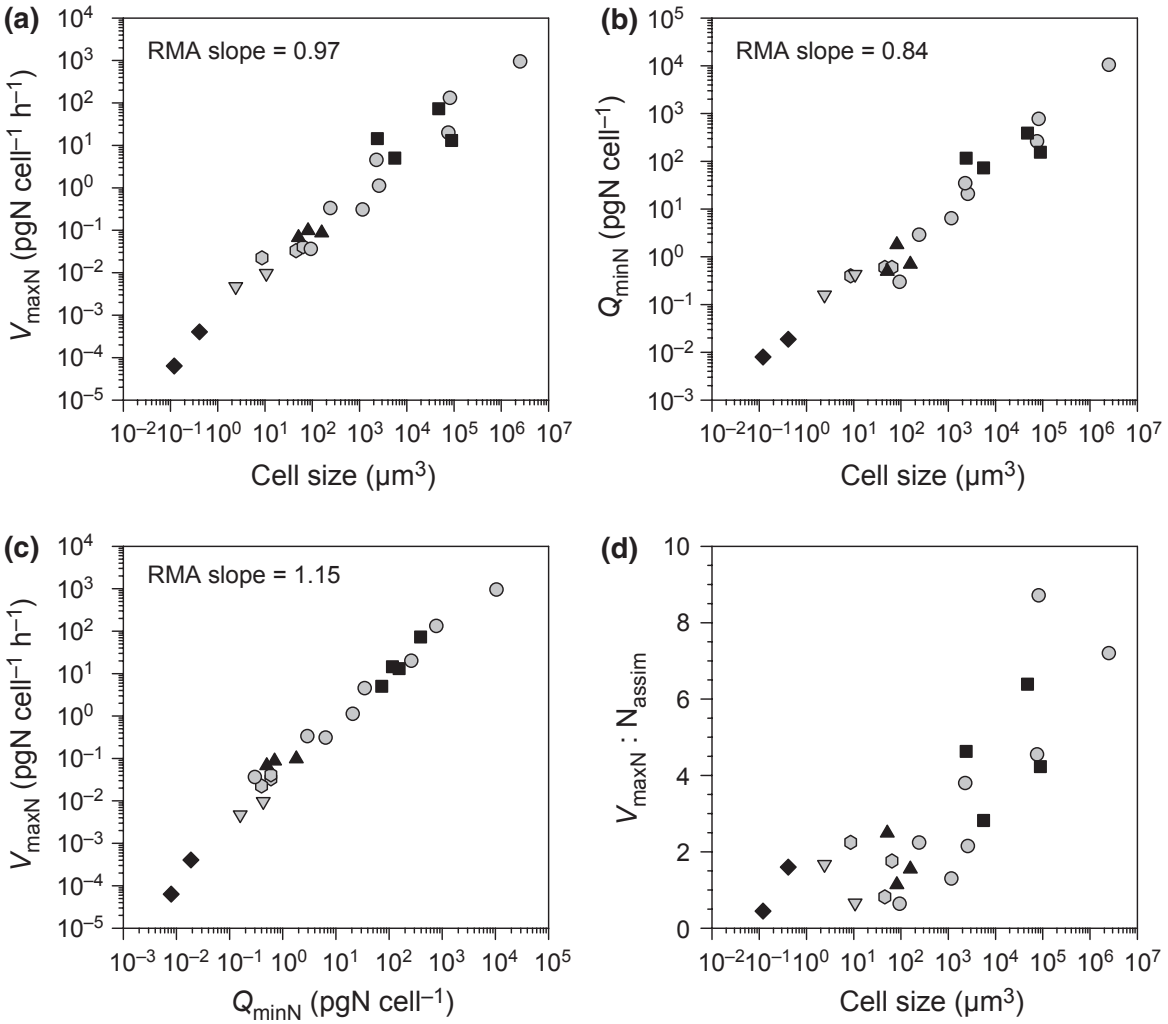

Figure 3 Size scaling of nutrient uptake and assimilation. (a) V_{maxN} vs. cell size, (b) Q_{minN} vs. cell size, (c) V_{maxN} vs. Q_{minN} and (d) the V_{maxN} : N_{assim} ratio vs. cell size. See Table 1 for data on each species and Table 2 for statistics. Symbols as in Fig. 1.

more slowly when acquiring nutrients and thus can sustain high uptake rates for longer periods of time (Stolte & Riegman 1995; Verdy *et al.* 2009). This strategy can be an advantage in environments where nutrient supply is highly intermittent (Falkowski & Oliver 2007).

Because the size-scaling exponent of V_{maxN} was higher than that of Q, and in addition both small and large cells showed similar growth rates, the V_{maxN}-to-N_{assim} ratio increased markedly with cell size. This observation contradicts the prediction that V_{maxN} : N_{assim} decreases with cell size, which rested on the assumption that V_{maxN} scales as the 2/3-power of V_{cell} (Verdy *et al.* 2009). Thus, in spite of their high V_{maxN} and storage capacity, the largest species in our study grew more slowly than the intermediate-size ones, because they had a smaller ability to convert nutrients into biomass. We speculate that, as cell volume increases, resources must cover a longer distance from the cell surface to the sites where they are metabolically processed, although this effect can be partially attenuated by the greater degree of vacuolation in larger cells (Raven 1995). The geometric constraints imposed by resource transportation networks (Banavar *et al.* 2002) may have resulted in a progressively slower supply rate of nutrients as phytoplankton cells become larger, which would explain the decrease in μ_{max} observed in the largest cells. Other factors, such as a decrease in the density of enzymatic units and/or a decrease in light absorption, may have contributed to cause the comparatively slow assimilation of nutrients into biomass, and hence slow growth rate, of large cells. In any event, our results show that V_{maxN} alone should not be regarded as a good predictor of μ_{max} in large phytoplankton because nutrient assimilation rather than nutrient uptake appears to be the most limiting step for growth in these cells.

We now examine the potential causes for the fact that small species also showed slower growth rates than intermediate-size cells. The C : N ratio decreased markedly in the species below 50 μm^3 in cell volume, which can be attributed to the increasing relative abundance of nitrogen-containing molecules that are part of non-scalable components, such as nucleic acids and membrane proteins (Raven 1994), as well as to a reduced storage of carbon-rich compounds such as lipids and carbohydrates. The smallest species were thus more nitrogen rich, but their V_{maxN} was, on a volume-specific basis, similar to that of larger cells. Therefore, μ_{max} of small species may have been more constrained, relative to that of intermediate-size cells, by their maximum nutrient uptake rate. In addition, non-scal-

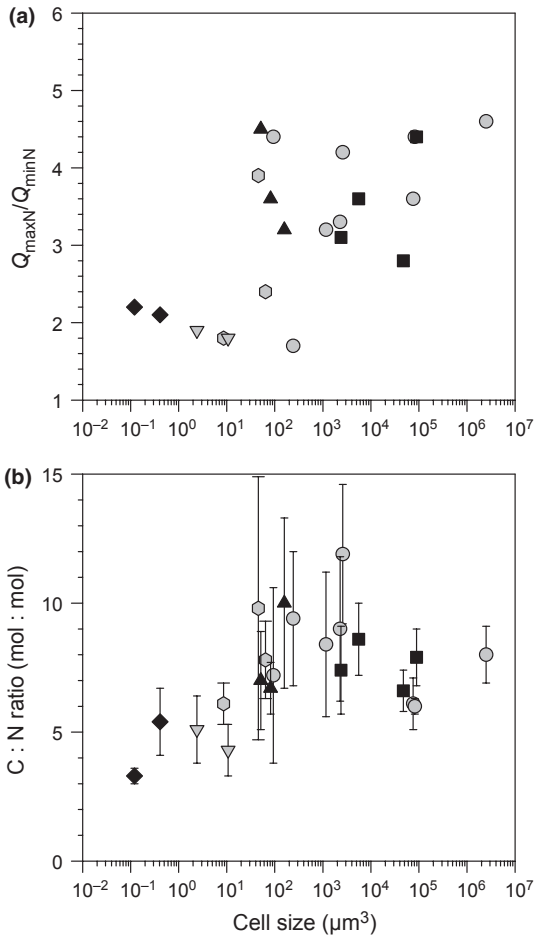

Figure 4 Cell-size dependence of phytoplankton elemental composition. (a) $\mathcal{Q}_{maxN}/\mathcal{Q}_{minN}$ vs. cell size. (b) Mean C:N ratio vs. cell size. Bars in (b) indicate ± 1 standard deviation. See Table 1 for data on each species. Symbols as in Fig. 1.

able components, such as membranes and nucleic acids, occupy an increasingly larger fraction of cell volume as cell size decreases, which causes a decrease in the fraction of cytoplasm available for other scalable, catalytic components directly involved in metabolic activity and biomass production (Raven 1994). Compared with larger cells, small cells would thus be slower in converting nutrients into biomass and as a result achieve lower maximum growth rates. A review of maximum growth rates in cultured cyanobacteria and chlorophytes did suggest a decrease in μ_{max} in the smallest cells but, presumably due to differences in growth conditions among studies, dispersion in the data was high (Raven 1994). Similarly, some field observations indicated the presence of unimodality in phytoplankton growth rates (Bec *et al.* 2008; Chen & Liu 2011), but lack of data on resource acquisition and metabolic processing prevented a direct examination of underlying mechanisms in these studies. Our measurements, all conducted under identical growth conditions, confirm the predicted decrease of μ_{max} in small cells and indicate that this effect becomes noticeable below a cell volume of *c.* 100 μm^3. Thus, we propose that a comparatively low nitrogen uptake ability (relative to requirements) together with a low efficiency in converting the acquired nitrogen into cell biomass may explain that small phytoplankton species have low μ_{max} and as a result are poor competitors in nutrient-rich environments.

A unimodal pattern in the size scaling of μ_{max} is relevant to understanding the dynamics of phytoplankton assemblages in the ocean. Due to the assumption that phytoplankton growth rates increase steadily with decreasing cell size, the seemingly paradoxical fact that phytoplankton blooms (defined as events of high biomass rather than high cell abundance) are rarely dominated by picophytoplankton has been traditionally attributed to the stronger grazing pressure suffered by small cells (Kiørboe 1993). Without denying a role for grazing, our results suggest that small phytoplankton are unlikely to dominate blooms simply because they have lower intrinsic growth rates than larger species. The unimodal pattern in μ_{max} also helps to explain why so many bloom-forming species are of intermediate cell size (Karentz & Smayda 1984; Johnsen *et al.* 1994). It has to be noted, however, that bloom-forming species such as diatoms often form chains, which means that, although their individual cell size may be in the nanophytoplankton size range, they are effectively part of the microphytoplankton size class. In addition, species above the intermediate-size range are expected to be more resistant to microzooplankton grazing and, therefore, even though their μ_{max} may not be as high as those of intermediate-size cells, they are also capable of forming blooms. The high storage capacity and high maximum nutrient uptake rate relative to requirements ($V_{max} : \mathcal{Q}_{min}$) of large cells make them especially well adapted for conditions of intermittent nutrient supply (Litchman *et al.* 2007). All these factors together explain the well-known dominance by microphytoplankton in highly productive marine environments (Chisholm 1992). The high storage capacity of the largest cells allows them to uncouple their growth from the dynamics of external nutrient supply, a scenario described by Droop's model (Droop 1973). In contrast, small cells have a comparatively small storage capacity and therefore their growth is tightly linked to the rate of external nutrient supply, as represented by Monod's model of microbial growth (Monod 1942). Finally, given that the size scaling of prey growth rate can affect the size scaling of consumers' abundance (DeLong & Vasseur 2012), the unimodal pattern in μ_{max} can also have implications for the size–abundance distribution of planktonic grazers, at least during the development of algal blooms.

The unimodal size scaling of μ_{max} and biomass-specific photosynthesis may also affect the relationship between cell size and species richness. According to models based on the kinetics of biochemical reactions, metabolic rate is a major factor controlling diversity (Allen *et al.* 2002) and rate of speciation (Allen *et al.* 2006). We could thus expect maximum species richness to occur at intermediate phytoplankton cell sizes, coinciding with the highest metabolic and growth rates. This prediction is supported by the analysis of a culture collection of *c.* 1000 phytoplankton species (Finkel 2008), which shows that the maximum species richness follows a log-normal function of cell size with a peak at around 100 μm^3. It must be noted that this data set may be subject to bias due to sampling and culturability issues as well as the presence of cryptic diversity (Finkel 2008). However, a field analysis of species richness across the nano- to microphytoplankton size range has also showed that the number of identified species peaks at intermediate cell sizes (Sabetta *et al.* 2005). The fact that both species richness and growth rates seem to be unimodal functions of cell size suggest that the connection between metabolic rate and phytoplankton evolutionary rates should be explored further.

It has been recently suggested that major evolutionary transitions are associated with changes in the size scaling of μ_{max} and R^M (De-

Long *et al.* 2010). According to this study, growth and metabolic rates increase with cell size in prokaryotes, are relatively size independent in protists and decrease with body size in metazoans. These shifts in size scaling would reflect the role of different constraints such as density of catalytic units and resource transport upon individual metabolic rate. Our experimental results show that, in a very broad sense, μ_{max} and R^M are roughly independent of cell size in photosynthetic unicells, given that both small and large species can sustain similar growth and metabolic rates. However, at a more detailed level, the size scaling of μ_{max} and R^M shifts from positive to negative as cell size increases. This transition does not require a change in cellular organisation, for example, from prokaryotes to eukaryotes, as the increase in growth and metabolic rates with cell size is already observed in the smallest eukaryotic species. Our results are consistent with the hypothesis that the unimodality in the size scaling of phytoplankton growth and metabolism, which is largely taxon independent, arises from a trade-off between several size-related constraints. These would include, for small cells, the elevated nitrogen requirements and, possibly, the limited availability of enzymes to convert nutrients into biomass; and, for large cells, the limitations imposed by resource transport from the cell membrane to metabolic processing sites. For small- to medium-size cells, we hypothesise that μ_{max} increases with V_{cell} because cells become less nitrogen rich and have progressively more space to accommodate catalysts involved in the synthesis of new biomass. In the medium-to-large cell-size range, μ_{max} would decrease with V_{cell} as a result of increasingly long intracellular distances for resource delivery, although other factors such as reduced light absorption may have also been involved. Our results suggest that the interplay between nutrient requirement, uptake and assimilation may control the size scaling of phytoplankton maximum growth rate, and the ability of species in different size classes to thrive under conditions of high resource availability and dominate biogeochemical cycling in the ocean.

ACKNOWLEDGEMENTS

We thank M. P. Lorenzo and A. Fernández for their help with laboratory work and S. Fraga for providing phytoplankton cultures. We also thank John P. DeLong and two anonymous referees for their helpful comments. This work was supported by the Spanish Ministry of Science and Innovation through research grant CTM2008-03699 (Macroecological patterns in marine phytoplankton) to E. M.

AUTHOR CONTRIBUTIONS

EM and PC designed the study; DCL-S and TR-R conducted the experiments and obtained data; CS, MH-O, JMB and JR obtained data; EM analysed the data and wrote the article, with substantial contributions from PC; all authors discussed the results and commented on the manuscript.

REFERENCES

Aksnes, D.L. & Cao, F.J. (2011). Inherent and apparent traits in microbial nutrient uptake. *Mar. Ecol. Prog. Ser.*, 440, 41–51.

Aksnes, D.L. & Egge, J.K. (1991). A theoretical model for nutrient uptake in phytoplankton. *Mar. Ecol. Prog. Ser.*, 70, 65–72.

Allen, A.P., Brown, J.H. & Gillooly, J.F. (2002). Global biodiversity, biochemical kinetics, and the energetic-equivalence rule. *Science*, 297, 1545–1548.

Allen, A.P., Gillooly, J.F., Savage, V.M. & Brown, J.H. (2006). Kinetic effects of temperature on rates of genetic divergence and speciation. *Proc. Natl. Acad. Sci. U.S.A.*, 103, 9130–9135.

Banavar, J.R., Damuth, J., Maritan, A. & Rinaldo, A. (2002). Supply-demand balance and metabolic scaling. *Proc. Natl. Acad. Sci. U.S.A.*, 99, 10506–10509.

Banse, K. (1976). Rates of growth, respiration and photosynthesis of unicellular algae as related to cell size: a review. *J. Phycol.*, 12, 135–140.

Banse, K. (1982). Cell Volumes, Maximal growth rates of unicellular algae and ciliates, and the role of ciliates in the marine pelagial. *Limnol. Oceanogr.*, 27, 1059–1071.

Bec, B., Collos, Y., Vaquer, A., Mouillot, D. & Souchu, P. (2008). Growth rate peaks at intermediate cell size in marine photosynthetic picoeukaryotes. *Limnol. Oceanogr.*, 53, 863–867.

Blasco, D., Packard, T.T. & Garfield, P.C. (1982). Size dependence of growth rate, respiratory electron-transport system activity, and chemical composition in marine diatoms in the laboratory. *J. Phycol.*, 18, 58–63.

Brown, J.H., Gillooly, J.F., Allen, A.P., Savage, V.M. & West, G.B. (2004). Toward a metabolic theory of ecology. *Ecology*, 85, 1771–1789.

Chen, B.Z. & Liu, H.B. (2011). Comment: Unimodal relationship between phytoplankton-mass-specific growth rate and size: A reply to the comment by Sal and Lopez-Urrutia (2011). *Limnol. Oceanogr.*, 56, 1956–1958.

Chisholm, S.W. (1992). Phytoplankton Size. In: *Primary Productivity and Biogeochemical Cycles in the Sea* (ed. Falkowski, PG). Plenum Press, New York and London, pp. 213–237.

Cullen, J., Yang, X. & MacIntyre, H.L. (1992). Nutrient limitation and marine photosynthesis. In: *Primary Productivity and Biogeochemical Cycles in the Sea* (ed. Falkowski, PG). Plenum Press, New York and London, pp. 69–88.

DeLong, J.P. & Vasseur, D.A. (2012). Size-density scaling in protists and the links between consumer–resource interaction parameters. *J. Anim. Ecol.*, 81, 1193–1201.

DeLong, J.P., Okie, J.G., Moses, M.E., Sibly, R.M. & Brown, J.H. (2010). Shifts in metabolic scaling, production, and efficiency across major evolutionary transitions of life. *Proc. Natl. Acad. Sci. U.S.A.*, 107, 12941–12945.

Droop, M.R. (1973). Some thoughts on nutrient limitation in algae. *J. Phycol.*, 9, 264–272.

Edwards, K.F., Thomas, M.K., Klausmeier, C.A. & Litchman, E. (2012). Allometric scaling and taxonomic variation in nutrient utilization traits and maximum growth rate of phytoplankton. *Limnol. Oceanogr.*, 57, 554–566.

Falkowski, P.G. & Oliver, M.J. (2007). Mix and match: how climate selects phytoplankton. *Nat. Rev. Microbiol.*, 5, 813–819.

Falkowski, P.G. & Owens, T.G. (1978). Effects of light intensity on photosynthesis and dark respiration in six species of marine phytoplankton. *Mar. Biol.*, 45, 289–295.

Fenchel, T. (1974). Intrinsic rate of natural increase: the relationship with body size. *Oecologia*, 14, 317–326.

Finkel, Z.V. (2001). Light absorption and size scaling of light-limited metabolism in marine diatoms. *Limnol. Oceanogr.*, 46, 86–94.

Finkel, Z.V. (2008). Does phytoplankton cell size matter? The evolution of modern marine food webs. In: *Evolution of aquatic photoautotrophs* (eds. Falkowski, PG & Knoll, AH). Academic Press, San Diego, pp. 333–350.

Finkel, Z.V., Irwin, A.J. & Schofield, O. (2004). Resource limitation alters the 3/4 size scaling of metabolic rates in phytoplankton. *Mar. Ecol. Prog. Ser.*, 273, 269–279.

Finkel, Z.V., Beardall, J., Flynn, K.J., Quigg, A., Rees, T.A.V. & Raven, J.A. (2010). Phytoplankton in a changing world: cell size and elemental stoichiometry. *J. Plankton Res.*, 32, 119–137.

Geider, R.J. (1992). Respiration: Taxation Without Representation? In: *Primary Productivity and Biogeochemical Cycles in the Sea* (ed. Falkowski, PG). Plenum Press, New York and London, pp. 333–360.

Gotham, I.J. & Rhee, G.Y. (1981). Comparative kinetic studies of nitrate-limited growth and nitrate uptake in phytoplankton in continuous culture. *J. Phycol.*, 17, 309–314.

Huete-Ortega, M., Cermeño, P., Calvo-Díaz, A. & Marañón, E. (2012). Isometric size-scaling of metabolic rate and the size abundance distribution of phytoplankton. *Proc. R. Soc. B*, 279, 1824–1830.

Johnsen, G., Samset, O., Granskog, L. & Sakshaug, E. (1994). In-vivo absorption characteristics in 10 classes of bloom-forming phytoplankton - taxonomic characteristics and responses to photoadaptation by means of discriminant and HPLC analysis. *Mar. Ecol. Prog. Ser.*, 105, 149–157.

Johnson, M.D., Voelker, J., Moeller, H.V., Laws, E., Breslauer, K.J. & Falkowski, P.G. (2009). Universal constant for heat production in protists. *Proc. Natl. Acad. Sci. U.S.A.*, 106, 6696–6699.

Karentz, D. & Smayda, T.J. (1984). Temperature and seasonal occurrence patterns of 30 dominant phytoplankton species in Narragansett Bay over a 22-year period (1959-1980). *Mar. Ecol. Prog. Ser.*, 18, 277–293.

Kiørboe, T. (1993). Turbulence, phytoplankton cell-size, and the structure of pelagic food webs. *Adv. Mar. Biol.*, 29, 1–72.

Kolokotrones, T., Savage, V., Deeds, E.J. & Fontana, W. (2010). Curvature in metabolic scaling. *Nature*, 464, 753–756.

Langdon, C. (1987). On the causes of interspecific differences in the growth-irradiance relationship for phytoplankton. Part 1. A comparative study of the growth-irradiance relationship of three marine phytoplankton species: Skeletonema costatum, Olisthodiscus luteus and Gonyaulax tamarensis. *J. Plankton Res.*, 9, 459–482.

Langdon, C. (1988). On the causes of interspecific differences in the growth-irradiance relationship for phytoplankton. II. A general review. *J. Plankton Res.*, 10, 1291–1312.

Laws, E.A. (1975). The importance of respiration losses in controlling the size distribution of marine phytoplankton. *Ecology*, 56, 419–426.

Legendre, L. & Rassoulzadegan, F. (1996). Food-web mediated export of biogenic carbon in oceans: Hydrodynamic control. *Mar. Ecol. Prog. Ser.*, 145, 179–193.

Litchman, E., Klausmeier, C.A., Schofield, O.M. & Falkowski, P.G. (2007). The role of functional traits and trade-offs in structuring phytoplankton communities: scaling from cellular to ecosystem level. *Ecol. Lett.*, 10, 1170–1181.

Marañón, E. (2008). Inter-specific scaling of phytoplankton production and cell size in the field. *J. Plankton Res.*, 30, 157–163.

Marañón, E., Cermeño, P., Fernández, E., Rodríguez, J. & Zabala, L. (2004). Significance and mechanisms of photosynthetic production of dissolved organic carbon in a coastal eutrophic ecosystem. *Limnol. Oceanogr.*, 49, 1652–1666.

Marañón, E., Cermeño, P., Rodríguez, J., Zubkov, M.V. & Harris, R.P. (2007). Scaling of phytoplankton photosynthesis and cell size in the ocean. *Limnol. Oceanogr.*, 52, 2190–2198.

Monod, J. (1942). *Recherches sur la croissance des cultures bacteriennes*. Hermann & Cie, Paris.

Raven, J.A. (1994). Why Are There No Picoplanktonic O_2 Evolvers with Volumes Less Than 10^{-19} M^3? *J. Plankton Res.*, 16, 565–580.

Raven, J.A. (1995). Scaling the seas. *Plant, Cell Environ.*, 18, 1090–1100.

Sabetta, L., Fiocca, A., Margheriti, L., Vignes, F., Basset, A., Mangoni, O. *et al.* (2005). Body size-abundance distributions of nano- and micro-phytoplankton guilds in coastal marine ecosystems. *Estuar. Coast. Shelf Sci.*, 63, 645–663.

Smith, R.E.H. & Kalff, J. (1982). Size-dependent phosphorus uptake kinetics and cell quota in phytoplankton. *J. Phycol.*, 18, 275–284.

Sommer, U. (1989). Maximal growth rates of Antarctic phytoplankton - only weak dependence on cell-Size. *Limnol. Oceanogr.*, 34, 1109–1112.

Stolte, W. & Riegman, R. (1995). Effect of phytoplankton cell size on transient-state nitrate and ammonium uptake kinetics. *Microbiology*, 141, 1221–1229.

Taguchi, S. (1976). Relationship between photosynthesis and cell size of marine diatoms. *J. Phycol.*, 12, 185–189.

Tang, E.P.Y. (1995). The allometry of algal growth rates. *J. Plankton Res.*, 17, 1325–1335.

Verdy, A., Follows, M. & Flierl, G. (2009). Optimal phytoplankton cell size in an allometric model. *Mar. Ecol. Prog. Ser.*, 379, 1–12.

SUPPORTING INFORMATION

Additional Supporting Information may be downloaded via the online version of this article at Wiley Online Library (www.ecologyletters.com).

Editor, Gregor Fussmann
Manuscript received 21 September 2012
First decision made 12 October 2012
Second decision made 11 November 2012
Manuscript accepted 14 November 2012